

Effect on Plasma Performance of a Single MHD Mode Feedback Control in Low-Aspect-Ratio RFP RELAX

Hiroyuki TANAKA, Sadao MASAMUNE, Seiya NAKAKI, Akio SANPEI, Kanae NISHIMURA, Ryosuke KODERA, Ryota UEBA, Go ISHII, Haruhiko HIMURA and Roberto PACCAGNELLA¹⁾

Kyoto Institute of Technology, Matsugasaki, Sakyo-ku, Kyoto 606-8585, Japan

¹⁾*Consorzio RFX, Associazione EURATOM-ENEA sulla Fusione, I-35127 Padova, Italy*

(Received 29 August 2013 / Accepted 12 March 2014)

A feedback control system for the stabilization of resistive wall mode (RWM) was applied to a low-aspect-ratio reversed field pinch (RFP) with minimum power supply capabilities to control the single mode. The system consists of 64 saddle coils (4 and 16 in poloidal and toroidal direction, respectively) in the actuator covering the whole torus on the outer surface of the vacuum vessel. The sensor coils also have the same structure. The saddle coils are connected in series to control the single $m/n = 1/2$ mode, which has the largest growth rate in RELAX. The radial component of the magnetic field from the sensor coils was suppressed to the preset level and the $m/n = 1/2$ magnetic mode, which otherwise grows with field penetration time of the vessel, was reduced to 0.1% of the edge poloidal field throughout the discharge. The RFP discharge duration has been extended to ~ 3.5 ms, the upper bound determined by the saturation of the iron core. Finally, the MHD control issues in a low-A machine are discussed.

© 2014 The Japan Society of Plasma Science and Nuclear Fusion Research

Keywords: reversed field pinch (RFP), resistive wall mode (RWM), active MHD control

DOI: 10.1585/pfr.9.1302057

Resistive wall mode (RWM) is an MHD instability which grows magnetic field diffusion time in the wall surrounding the plasma [1]. Sometimes, the RWM degrades the plasma performance in toroidal fusion plasmas. In tokamaks, the pressure-driven $m = 1$ kink mode is predicted to limit the achievable normalized beta [2]. The stabilization of the RWM is critical in high performance tokamak plasmas [3]. In reversed field pinches (RFPs), when operated with a resistive shell, the combined effect of the growth of the current-driven non-resonant kink mode and the associated distortion of the magnetic boundary conditions brought about by the RWM tends to limit the discharge duration. The distorted magnetic boundary conditions tend to enhance the nonlinear interaction of the resonant tearing modes, resulting in degraded RFP plasma performance [4]. Thus, active control or stabilization of the RWM is quite important for achieving high-performance fusion plasmas.

It was demonstrated in Extrap-T2R RFP that the stabilization of the RWM has resulted in improved plasma performance with discharge duration up to \sim twenty times the magnetic field diffusion time of the resistive shell [5]. In fact, the duration was limited by the iron core saturation or the power supply capability. In the RFX-mod experiment, they succeeded in stabilizing RWM and suppressing the locked mode, which made it possible to run the machine with plasma current up to 2 MA [6]. The effect of active

MHD control is remarkable when we compare the case without feedback. Without the feedback stabilization of RWM, the plasma current was restricted to ~ 0.6 MA owing to the localized heat load to the wall brought about by the locked mode. The feedback stabilization of RWM by the saddle coil arrays covering the whole torus in RFP machines was success. Thus, the next important concern is to identify the minimum coverage of the actuator coils for the effective stabilization of the RWM [7]. Moreover, from the viewpoint of system maintenance and power consumption in the control system, it is also important to seek simpler control schemes.

RELAX is a low-aspect-ratio (low-A) RFP whose major objectives include studies of MHD-mode dynamics [8]. It has been analytically shown that the current-driven kink mode with $m = 1$, $|n|(a/R) \sim 1$, either internally non resonant or externally non resonant depending on the current profile, has the largest growth rate as an RWM [9]. In addition, it was experimentally demonstrated that the maximum discharge duration in RELAX was limited by the growth of the $m/n = 1/2$ externally non-resonant kink mode to 1-2% of the edge poloidal field [10]. In the present experiment, we have attempted to control the RWM with minimum power supply capability, and to identify the issues of active MHD control associated with the low-A characteristic of the machine.

RELAX is a low-A RFP machine using a 4-mm thick stainless steel vacuum vessel with a major radius R of 0.5 m, a minor radius a of 0.25 m, and an aspect ratio

author's e-mail: tanaka11@nuclear.es.kit.ac.jp; masamune@kit.ac.jp

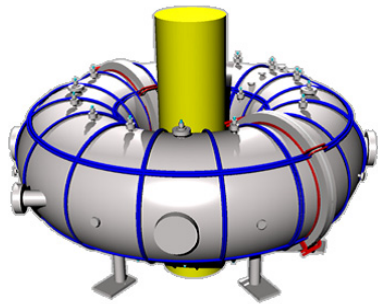


Fig. 1 Saddle coil array for the actuator and sensor for active MHD control in RELAX.

$A = R/a$ of 2. We have operated the machine without an outer conducting shell; therefore, the vessel acts as a resistive wall with the field penetration time of ~ 1.5 ms [11]. The operational regions of RELAX plasmas can be summarized as follows: plasma current I_p from 40 to 125 kA, line-averaged electron density from 0.2 to $\sim 2 \times 10^{19} \text{ m}^{-3}$ [12], and central electron temperature from ~ 60 to ~ 150 eV [13].

The magnetic diagnostics are the following. Toroidal arrays of magnetic probes are attached at the top and bottom inside the vacuum vessel. Each array consists of 14 pick-up coils. Fast magnetic fluctuations of even and odd poloidal mode numbers are provided by these arrays. In addition, toroidal arrays of 16 sine and cosine B_r coils are attached on the outer surface of the vessel. These arrays provide slowly varying $m = 1$ magnetic signals outside the vessel. We have used signals from these two outer arrays to identify the resistive wall mode.

Figure 1 shows the sensor and actuator coils in RELAX. An array of 64 saddle coils, divided into 4 in the poloidal direction and 16 in the toroidal direction, completely covers the outer surface of the vacuum vessel. The actuator coils also have the same structure as the sensor coils. In the present experiment, we concentrated our attention on controlling or stabilizing only the single mode to observe the effect on plasma performance and to identify problems associated with the low- A nature of the machine. The sensor and actuator saddle coils are connected to form two pairs of helical coils having the $m/n = 1/2$ structure, as shown in Fig. 2. A controlled power supply system was assigned to each pair to control the orthogonal $m = 1$ components. For this type of sensor/actuator connection, difficulties may arise in controlling the $m = 1$ component in low- A configuration, which will be discussed later.

The block diagram for the feedback control system is shown in Fig. 3. An H-bridge circuit using four IGBTs, was adopted to control the radial component of the edge magnetic field on the outer surface of the vacuum vessel. When the $m/n = 1/2$ sensor coil signal exceeds a certain preset threshold level, two of the four IGBTs are driven to feed the actuator coils with current until the sensor coil sig-

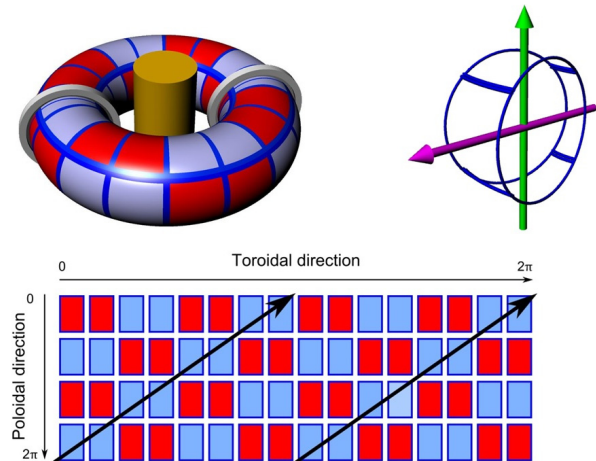


Fig. 2 Schematic view of the 64 saddle coils covering the entire torus, and their connection to produce the $m/n = 1/2$ control fields. The bottom figure shows the envelope of the coil surface showing that the blue coils are connected in series in the direction of the arrow. The blue and the red coils produce orthogonal $m = 1$ control fields.

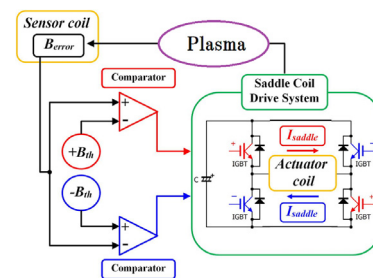


Fig. 3 Block diagram for the sensor and actuator circuit in the controller.

nal is suppressed below the threshold level. In the present control system, we have adopted a simple on-off control scheme. The actuator current rise rate is controlled by the charging voltage of a capacitor connected to the IGBTs. The voltage is optimized to minimize the effect of overshooting and to have an appropriate response time for the single $m/n = 1/2$ RWM. Two pairs of sensor and actuator coils can suppress the growth of the single $m/n = 1/2$ mode, because the RW kink mode is stable when the ideal wall boundary condition ($B_r(a) = 0$) is satisfied.

One of the problems associated with the saddle coil array is the so-called sideband effect produced by a set of discrete coils [14]. Figure 4 shows the toroidal mode spectrum of the $m = 1$ external magnetic field produced by the saddle coil array in the experiment. As designed, the dominant component of the external field is $m/n = 1/2$, and at the same time the $m/n = 1/-6$ component with a significant amplitude was also produced. The $m/n = 1/-6$ component is an internally resonant perturbation to the RELAX RFP if

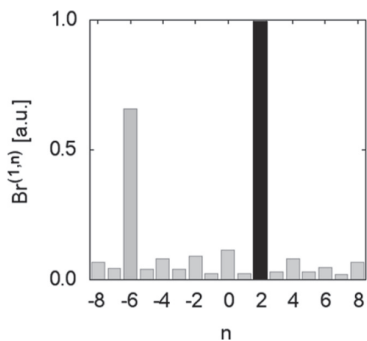


Fig. 4 Toroidal mode spectrum measured with the sine and cosine B_r coil arrays produced by the actuator coils connected in series to form the $m/n = 1/2$ structure.

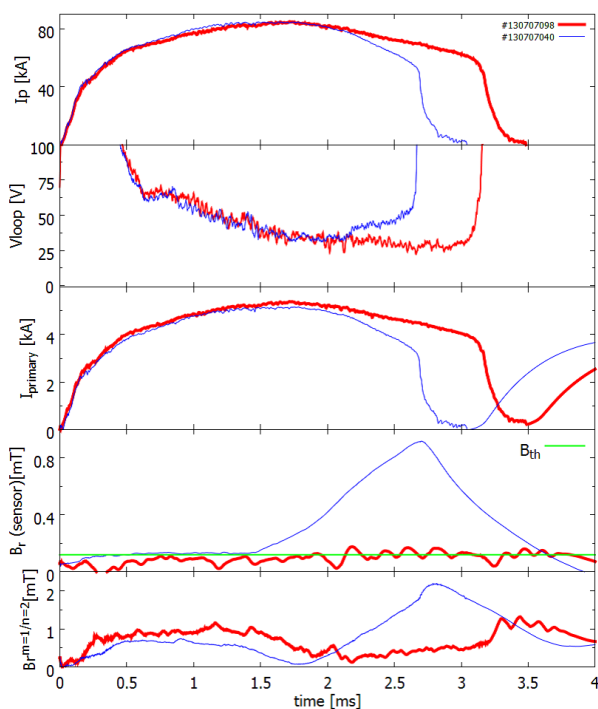


Fig. 5 Time evolutions of I_p , V_{loop} , $I_{primary}$, B_r sensor signal, and $m/n = 1/2$ amplitude from the sine and cosine B_r array, without (blue) and with (red) active control.

it penetrates into the plasma to reach the $q = -1/6$ resonant surface.

Another problem may be the interaction between the two orthogonal sensor/actuator saddle coil arrays. The mutual inductance between these two arrays was measured less than $2 \mu\text{H}$, which should be compared with the self-inductance ($\sim 220 \mu\text{H}$) of each coil. In the connection of the saddle coils for the single-mode control, the crosstalk or interaction between the two orthogonal arrays will have negligible effect on the control scheme.

In Fig. 5, we have compared the time evolution of the plasma current I_p , the loop voltage V_{loop} , the primary cur-

rent $I_{primary}$, and the sensor coil signals together with the threshold level of the $m/n = 1/2$ mode amplitudes in discharges with and without feedback control. It is clear that the $m/n = 1/2$ mode, measured with the toroidal array of the sine-cosine coils for B_r , grows with the field penetration time of the vacuum vessel without the control. As the mode grows, the plasma current tends to slightly decrease, followed by a rapid decrease to terminate the discharge when the mode grows to 2% of the edge poloidal field. In addition, one can observe that the sensor coil signal shows almost the same evolution as that of the $m/n = 1/2$ mode.

Without feedback, one can observe the enhanced loop voltage slightly after the current peak, namely after ~ 2 ms. Because the RWM of interest is in the externally non-resonant kink mode, its growth accompanies the global deformation of the plasma. The deformation can cause the magnetic field lines to penetrate into the vacuum vessel, or the resistive wall. The loop voltage in the RFP can be explained by the helicity balance model [15]. When the field lines intersect the surrounding wall, the potential difference between two footpoints can cause enhanced helicity loss, resulting in enhanced loop voltage. The observed enhanced loop voltage can be attributed to the enhanced helicity loss associated with the growth of RWM. The discharge duration without the RWM feedback is determined by the iron core saturation well before the current termination, which results from the enhanced loop voltage associated with the growth of RWM.

When feedback control is applied, the growth of the $m/n = 1/2$ mode significantly decreases and longer discharge duration up to ~ 3.5 ms is achieved. The sensor array signal is reduced below the preset threshold amplitude, as is clear from the figure. On the other hand, the edge radial field, measured with the sine-cosine coil arrays, shows that the $m/n = 1/2$ mode amplitude increases about twice as much as that without feedback before the growth of the mode after ~ 1.5 ms. The time evolution of the global discharge parameters, such as the loop voltage and plasma current, is not influenced by the increased amplitude. The mode amplitude remained below $\sim 0.5\%$ throughout the discharge duration owing to the feedback control of the mode. As shown in the third box in Fig. 5, when the feedback is applied, the primary current starts increasing during the current decreasing phase without decreasing to zero at the plasma current termination. This indicates that the discharge duration is not controlled by the growth of the particular MHD mode but by the saturation of the iron core when feedback is applied. The degradation of the discharge in the final phase is explained in the following manner. As the flux consumption increases toward the limit (~ 0.24 Vs), the fraction of the magnetization current in the primary current increases, and the vertical field produced by the magnetization current negatively affects the equilibrium. Then, the discharge termination follows. When feedback is applied, the discharge duration is lim-

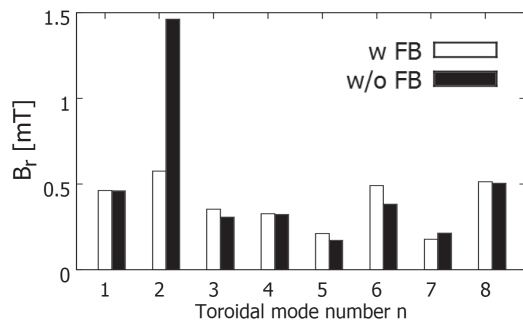


Fig. 6 Comparison of the toroidal mode spectrum of B_r from sine and cosine coil arrays at $t = 2.5$ ms. The amplitude of the $m/n = 1/2$ component decreased by $\sim 1/3$ with feedback.

ited by the iron core saturation without the loop voltage enhancement associated with the growth of RWM.

The reason for the increase in the $m/n = 1/2$ component (measured with sine and cosine B_r arrays) with feedback is attributed to the following. For the single-mode control, the sensor and actuator saddle coils are connected to form the same structure as that of the target mode. In the actual situation, the $m = 1$ component is produced by the top and bottom saddle coils for the vertical field, and the inboard and outboard side saddle coils for the horizontal component. In the low-aspect-ratio configuration, the area of the inboard side saddle coil is much smaller than the outboard side saddle coil, and the current flows to both coils connected in series. As a result, higher harmonics components ($m/n = 2/4$, and so on) are produced when the actuator coil current is driven. The actuator current is driven from the start of the discharge to compensate for the sensor signal, which comes from the saddle coils connected in the same manner as the actuator coils. Therefore, the sensor coil signal is suppressed below the threshold level through the discharge, whereas the $m/n = 1/2$ mode amplitude measured with the sine and cosine arrays increases during the discharge. Note that the resolution of the poloidal and toroidal mode numbers is not high enough to identify the higher harmonics of the $m/n = 1/2$ component in the present magnetic probe array.

In Fig. 6, we compare the $m = 1$ mode spectrum at $t = 2.5$ ms measured with the toroidal arrays of sine and cosine B_r coils. It is clear that only the $m/n = 1/2$ mode is suppressed to the same level as the remaining modes. Figure 7 shows the toroidal mode spectrum at $t = 2.5$ ms measured with the toroidal array of edge magnetic probes inside the vacuum vessel. Because the probes are located only at the top and bottom, we cannot identify the sign of the toroidal mode number. It is clear that the $m/n = 1/4$ mode is dominant and the mode amplitude decreases toward higher n , which is typical of internally resonant tearing modes. Note that we cannot observe the growth of the $m/n = 1/2$ mode without feedback because we have applied high-pass filters

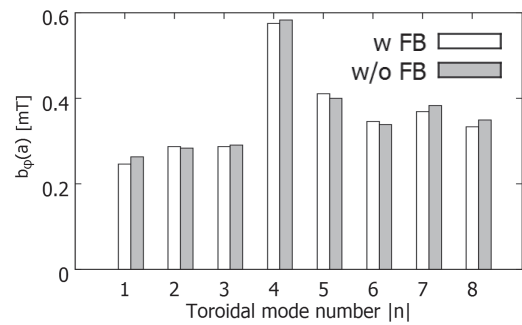


Fig. 7 Comparison of the toroidal mode spectrum of b_ϕ from the edge magnetic probes inside the vacuum vessel. No significant effect of feedback is observed in the edge magnetic fluctuations.

in calculating the mode spectrum to suppress the effect of low-frequency components mainly arising from the change in equilibrium. The growth of the $m/n = 1/2$ mode is slow; hence, the $m/n = 1/2$ mode amplitude cannot be identified by the edge magnetic probes inside the vacuum vessel. We need to point out that the $m/n = 1/6$ (-6 for internally resonant component) does not significantly increase when the feedback is activated.

The results have shown that the growth of the single RWM can be suppressed to low amplitudes by two pairs of saddle coil arrays driven by two independent power supplies. The suppression of the RWM amplitude has led to improved plasma performance mainly to longer discharge duration up to the limit set by the iron core saturation.

Acknowledgments

This work was financially supported with KAKENHI Grant Number 22360390 and the NIFS Collaboration program (NIFS07KOA022).

- [1] D. Phirsch and H. Tasso, Nucl. Fusion **11**, 259 (1971).
- [2] E.J. Strait, Phys. Plasmas **1**, 1415 (1994).
- [3] M. Okabayashi *et al.*, Nucl. Fusion **45**, 1715 (2005).
- [4] S. Ortolani and RFX team, Plasma Phys. Control. Fusion **48**, B371 (2006).
- [5] P.R. Brunzell *et al.*, Phys. Rev. Lett. **93**, 225001 (2004).
- [6] P. Martin *et al.*, Nucl. Fusion **51**, 094023 (2011).
- [7] M. Baruzzo *et al.*, Nucl. Fusion **52**, 103001 (2012).
- [8] S. Masamune *et al.*, Trans. Fusion Sci. Technol. **51** (2T), 197 (2007).
- [9] S. Masamune, M. Iida and H. Oshiyama, J. Phys. Soc. Jpn. **68**, 2161 (1999).
- [10] S. Masamune *et al.*, Proc. 22nd IAEA Fusion Energy Conf., Geneva, EX/7-IRB (2008).
- [11] S. Masamune *et al.*, J. Phys. Soc. Jpn. **76**, 123501 (2007).
- [12] M. Sugihara *et al.*, Plasma Fusion Res. **5**, S2061 (2010).
- [13] S. Masamune *et al.*, Proc. 24th IAEA Fusion Energy Conf., San Diego, EX/P4-24 (2012).
- [14] R. Paccagnella *et al.*, Nucl. Fusion **42**, 1102 (2002).
- [15] T.R. Jarboe and B. Alper, Phys. Fluids **30**, 1177 (1987).